Using a Nonlinear Controller to Optimize a Variable Speed Wind Power System

Iulian MUNTEANU, Nicolaos A. CUTULULIS, Antoneta BRATCU and Emil CEANGĂ

Advanced Control Systems Research Centre, „Dunărea de Jos" University of Galați
47 Domnească, 800008–Galați, Romania
Phone/Fax: (+40) 2 36 46 01 82; E-mail: Iulian.Munteanu@ugal.ro

***Abstract* – In this paper an optimal control structure for variable speed fixed pitch wind turbines is presented. The frequency separation of the short term and the long term variations, adopted in the wind modeling, has resulted in a two loops control structure. The low frequency loop is based upon a nonlinear (on-off) controller, and the high frequency loop results from a LQ stochastic problem. The proposed approach allows to using the advantages of the on-off control (i.e. robustness), while realizing a trade-off between the energy conversion maximization and the control input minimization that determines the mechanical stress of the drive train. The effectiveness of the whole structure was tested on an electromechanical wind turbine simulator.**

***Index Terms* – Wind energy, variable speed operation, on-off control, linear quadratic optimization**

I. INTRODUCTION

The wind energy conversion systems (WECS) based on variable speed fixed pitch horizontal axis wind turbines (HAWT) are generally controlled in the sense of maximizing the energy captured from the wind. This task is accomplished by the **control subsystem** which manages the variable speed operation of the wind turbine, adjusting the aerodynamic efficiency of the fixed pitch wind turbine. This efficiency is expressed by the power coefficient, C_p, which presents a maximum value for a well-determined tip speed ratio, λ_{opt} (fig. 1), implying that the power characteristic of the wind turbine has a maximum for each wind speed (fig. 2). All these maxima form the so-called *optimal regimes characteristic* (ORC), as illustrated in fig. 2.

If λ_{opt} is known, the (optimal) control may be implemented by tracking the corresponding value of the shaft speed, like in [1].

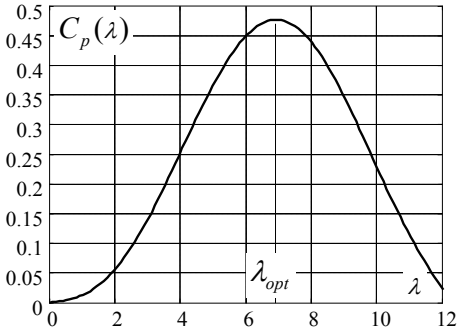

Fig. 1. The power coefficient vs. the tip speed

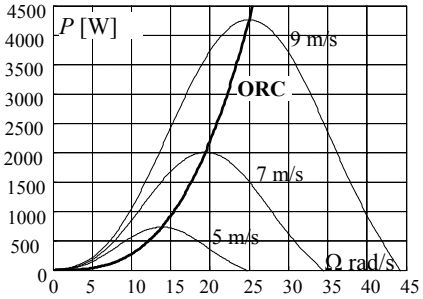

Fig. 2. The optimal regimes characteristic (ORC)

When the value of λ_{opt} is not known, the control objective is defined as tracking the maximum of the power characteristics (fig. 2).

In the literature, various methods are proposed for maximizing the power harvested from the wind. For example, this is the case of the so called "Maximum Power Point Tracking" (MPPT) controller, which uses minimal information from the system [2], and of the fuzzy control techniques [3], yielding more flexible, but quite context dependent controllers. The sliding mode techniques have been also used for controlling the generated power [4].

All the above listed methods have as exclusive goal the maximization of the energetic efficiency, while ignoring the large torque variations, related to the system's reliability. This aspect has been considered in [5] and [6], by imposing the minimization of the generator torque variations, $\Delta\Gamma_G(t)$, which results in the mechanical fatigue reduction of the drive train. In this case, the control subsystem solves a Gaussian linear quadratic (LQG) optimization problem [7] – associated with the liniarized aerodynamic subsystem – expressed by a combined criterion:

$$I = E\left\{\alpha \cdot \left[\lambda(t) - \lambda_{opt}\right]^2\right\} + E\left\{\Delta\Gamma_G^2(t)\right\}, \qquad (1)$$

where $E\{\cdot\}$ is the statistical average symbol and the positive coefficient α makes the trade-off between the energetic efficiency and the mechanical stress.

The linearized system's parameters depend on the operating point (wind speed); this aspect has been considered by using a gain scheduling adaptive structure, combined with a Kalman filter for state reconstruction.

Starting from the frequency separation principle in the wind speed, introduced in [8], this paper proposes a control subsystem, which optimizes the combined criterion (1) with no use of adaptive structures. The control algorithm relies upon separating the seasonal (low frequency) and the turbulence (high frequency) wind speed components from the Van der Hoven wind model [9]. As consequence, the proposed control structure is formed by two loops, separately driven respectively by the two components of the wind. One loop is built to reach the stationary optimal conversion regime using a nonlinear (on-off) controller, and the second loop is designed to optimize the dynamic regime of the wind turbine, using a LQG controller.

The rest of the paper is organized as follows. In the next section is presented the modeling of the wind energy conversion system. Section III states the control problem and details the general two loops control structure. The proposed control subsystem has been tested on a real time electromechanical simulator, described in section IV. Some experimental results, concerning both of the control loops, are discussed in section V. The concluding remarks end this paper.

II. MODELLING

The variable speed WECS (fig. 3) is formed by: the wind turbine (the aerodynamic subsystem, S_1), the gearbox (S_3), the electromagnetic subsystem (the asynchronous machine and the static converter, S_2) and the control unit (S_4).

The aerodynamic subsystem (S_1 in fig. 3) is modeled like in [10], by the nonlinear wind torque characteristic, $\Gamma_{wt}(\Omega, v)$:

$$\Gamma_{wt} = \frac{1}{2} \cdot \pi \cdot \rho \cdot R^3 \cdot v^2 \cdot \underbrace{\frac{C_p(\lambda)}{\lambda}}_{C_\Gamma(\lambda)}, \tag{2}$$

where ρ is the air density, R is the blade length, Ω is the rotational speed of the low-speed shaft, v is the wind speed, λ is the tip speed ratio, given as:

$$\lambda = \frac{R \cdot \Omega}{v}, \tag{3}$$

$C_p(\lambda)$ is the power coefficient, as a polynomial of λ (like in fig. 1) [11], and $C_\Gamma(\lambda)$ is the torque coefficient.

The electromagnetic subsystem (S_2 in fig. 3) yields the electromagnetic torque, Γ_G, in response to a torque control scheme. The vector control is used as a dynamic compensator of the electric machine. Therefore, the dynamics of S_2 can be approximated by those of a first order filter:

$$H_g(s) \overset{\Delta}{=} \frac{\Gamma_G^*(s)}{\Gamma_G(s)} = \frac{1}{T_g s + 1}, \tag{4}$$

where T_g is negligible versus that of the drive train (S_3 in fig. 3).

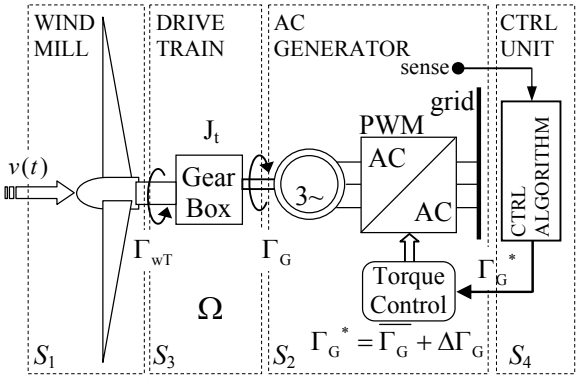

Fig. 3. Wind power system's structure

The electromechanical subsystem interacts with the turbine rotor through the drive train; the dynamics of this latter is expressed by:

$$J_t \cdot n \cdot \frac{\mathrm{d}\Omega}{\mathrm{d}t} = \frac{\Gamma_{wt}}{n} - \Gamma_G, \tag{5}$$

where n is the ratio of the gear-box and J_t expresses the total inertia of the turbine, referred to the high-speed shaft.

The control unit (S_4 in fig. 3) provides the electric generator torque reference, according to a control algorithm.

The wind model is added to the general model of the system. The wind can be modeled as a stochastic process with two components (fig. 4), like in [9]: the *seasonal*, slowly variable component, $\bar{v}$, and the *turbulence*, rapidly variable component, $\Delta v(t)$:

$$v(t) = \bar{v} + \Delta v(t) \tag{6}$$

The low frequency component, $\bar{v}$, determines the average position of the operation point on the wind turbine characteristic, and $\Delta v(t)$ generates the high frequency variations around this point. This high frequency component is modeled as a zero mean stochastic process obtained by coloring a white noise with a first order filter having the time constant T_w.

The nonlinear model (5) is linearized around the operating point corresponding to the maximal energy conversion efficiency, characterized by λ_{opt}.

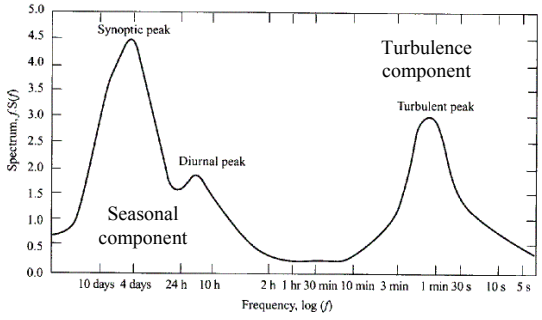

Fig. 4. Van der Hoven wind model [12]

For a variable x of the model, the following notations are adopted:

$$\bar{x} = x\big|_{\text{optimal operating point}} \; ; \; \Delta x = x - \bar{x} \; ; \; \overline{\Delta x} = \frac{\Delta x}{\bar{x}}$$

Starting from the nonlinear aerodynamic characteristic (2), one obtains the linearized dynamic model of the turbine, as deduced in [13]:

$$\begin{cases} \underline{\dot{x}}(t) = A \cdot \underline{x}(t) + B \cdot u(t) + L \cdot e(t) \\ \underline{z}(t) = C \cdot \underline{x}(t) \end{cases}, \tag{7}$$

where $\underline{x}(t) = \left[\overline{\Delta\Omega}(t) \quad \overline{\Delta\Gamma}_{wt}(t) \right]^T$ is the state vector, $u(t) = \overline{\Delta\Gamma_G}$ is the control input and the output (measure) variable is defined as being the normalized variation of the tip speed ratio: $z(t) = \overline{\Delta\lambda}(t) = \Delta\lambda / \bar{\lambda}$. Matrices in the above model are:

$$\left.\begin{aligned} A &= \begin{bmatrix} 0 & 1 \\ \dfrac{\gamma}{T_w} & \dfrac{\gamma}{J_T} - \dfrac{1}{T_w} \end{bmatrix} \qquad B = \begin{bmatrix} -\dfrac{1}{J_T} \\ -\dfrac{\gamma}{J_T} \end{bmatrix} \quad L = \begin{bmatrix} 0 \\ \dfrac{2-\gamma}{T_w} \end{bmatrix} \\ C &= \begin{bmatrix} \dfrac{2}{(2-\gamma)} & -\dfrac{1}{(2-\gamma)} \end{bmatrix} \end{aligned}\right\}, \tag{8}$$

where $J_T = \bar{\Omega} \cdot J_t \big/ \overline{\Gamma_{wt}}$ has significance of time constant and:

$$\gamma = \gamma(\bar{\lambda}) = \frac{C_p^{'}(\bar{\lambda}) \cdot \bar{\lambda} - C_p(\bar{\lambda})}{C_p(\bar{\lambda})} \tag{9}$$

is a parameter introduced in [6], which has the value of (–1) for λ_{opt}; this parameter presents large variations with the wind speed. Relation (8) shows that all the liniarized system's parameters depend on the operating point or, equivalently, on the seasonal wind speed, $\bar{v}$. It can be shown that J_T and T_w are inversely proportional with $\bar{v}$. As for γ, it is practically impossible to compute its value, if the information about $C_p(\lambda)$ is poor or difficult to obtain (see (9)). Therefore, the system is variant in relation to the seasonal wind speed, which is an inconvenient for the control design.

III. The Control Structure

The control structure results from considering that the two components of the wind speed (6) drive two kinds of the system's dynamics: the *low frequency* dynamics are excited by the seasonal component, $\bar{v}$, which determines the average position of the operation point on the wind turbine characteristic, whereas $\Delta v(t)$ generates the *high frequency* variations around this point [13].

This approach, called *the frequency separation principle*, supposes the separate compensation of the two dynamics [8].

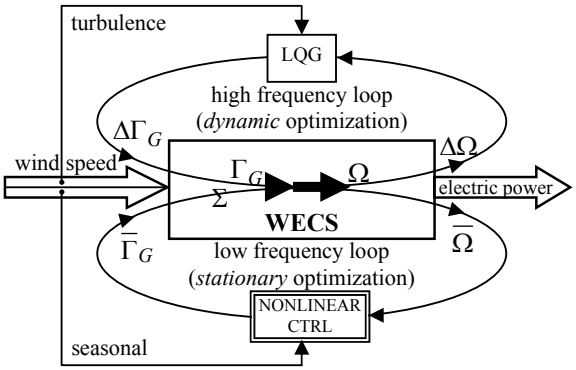

Fig. 5. Frequency separation principle

A nonlinear controller, using the seasonal component, is designed to drive and maintain the system *at* an operating point on the optimal regimes characteristic, whereas a LQ controller, using the turbulence component, is computed to optimize the linearized system's behavior *around* this point.

Fig. 5 presents the two loops of the proposed control structure, separately driven by the two components of the wind speed: the low frequency loop (LFL) and the high frequency loop (HFL).

A. LFL: The control problem

The control problem associated with the LFL concerns the *stationary* optimization, which means to operate a wind turbine at variable speed such that its operating point stay on the ORC. This is equivalent to maintaining the power coefficient, C_p, which depends on the *tip speed ratio*, λ, at its maximal value, $C_p(\lambda_{opt})$ (see fig. 1). This is realized by tracking the wind torque corresponding to λ_{opt}, as to (2):

$$\Gamma_{wt}(\lambda_{opt}) = 0.5 \cdot \pi \cdot \rho \cdot R^3 \cdot C_\Gamma\left(\lambda_{opt}\right) \cdot \bar{v}^2 \tag{10}$$

In the above relation it is the seasonal component of the wind speed, $\bar{v}$, that occurs, as this one determines the (slowly) variation of the operating point.

B. LFL: The proposed structure

The LFL achieves the stationary optimization, that is, the maximal power tracking, using the seasonal component, which establishes the operating point. Fig. 6 presents the detailed scheme of this loop, which is commented below.

The *seasonal* component, $\bar{v}(t)$, is extracted from the wind speed, $v(t)$, by a low-pass filter of fourth order, whose cutoff frequency must be at most the drive train's bandwidth. The output of the filter is used by a nonlinear controller to zeroing the difference λ-λ_{opt}. *That implies that the mostly variable parameter of the system, γ, is constant and the linearized system* (7) *is invariant in relation to this parameter.*

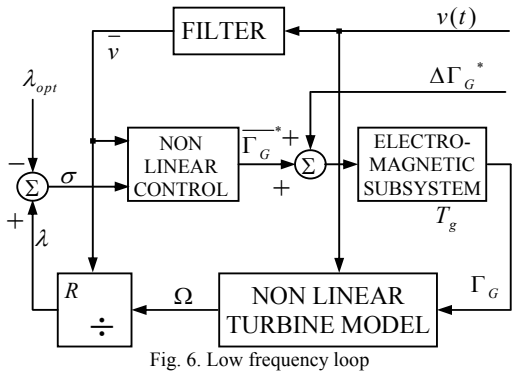

Fig. 6. Low frequency loop

Fig. 7 details the nonlinear controller structure. The controller output has two terms:

$$u_{NL} = u_m + u_N ,$$

where u_m is the *quasi-continuous* component (slowly variable, as it depends proportionally with the square of the seasonal wind speed, $\bar{v}(t)^2$) and u_N is an *alternative* component, resulted from switching between two values, $+\beta$ and $-\beta$, adjustable in the range of maintaining the system's stability. Therefore, the global nonlinear control input is, in fact, the superposition of an "equivalent" control and of an on-off control having good properties of robustness:

$$u_{NL} = C \cdot \bar{v}^2 + \beta \cdot \text{sign}\left(\underbrace{\sigma(t)}_{\lambda - \lambda_{opt}} \right), \tag{11}$$

where $C = 0.5 \cdot \pi \cdot \rho \cdot R^3 \cdot C_\Gamma\left(\lambda_{opt}\right)$. u_{NL} represents the *static* component of the electromagnetic torque, $\overline{\Gamma_G}$, ensuring to reach the "static" optimal operating point on the $C_p(\lambda)$ characteristic.

Because the electromagnetic subsystem behaves as a first order filter, as shown in (4), it is necessary to introduce a sample-and-hold element (S&H) to control the commutation frequency of u_N. As a consequence, the amplitude of Γ_G is smaller than β.

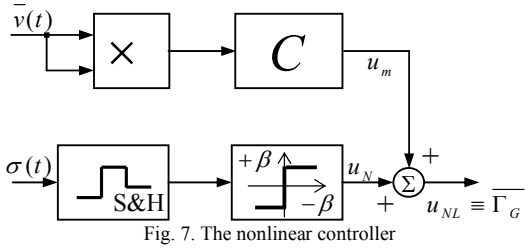

Fig. 7. The nonlinear controller

C.HFL: The control problem

As the turbine is highly inertial versus the wind speed variation, a control exclusively based on the stationary optimization could be harmful to the mechanical subsystems (to the gear-box for example), because of the large torque variations involved.

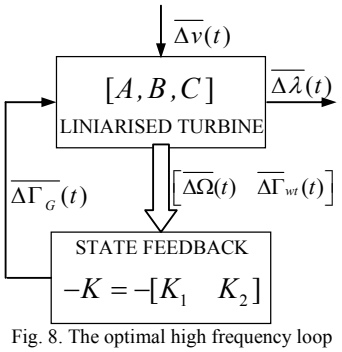

Fig. 8. The optimal high frequency loop

Therefore, an optimization criterion of form (1), whose second term expresses the *minimization* of the *torque control variations*, is suitable to meet the reliability requirements. This is called *dynamic* optimization and may be formulated as a *LQG* optimization problem, as shown in [13].

Taking into account the above definition of the state model, the performance index (1) reflects a trade-off between the output variable variations' minimization and the control input variations' minimization and can be put into the form:

$$I = E\left\{ \underline{x}^T(t) \cdot \left(C_\alpha^T \cdot C_\alpha \right) \cdot \underline{x}(t) + u^T(t) \cdot R \cdot u(t) \right\} \rightarrow \min , \tag{12}$$

where $R = 1$ and $C_\alpha = \sqrt{\alpha} \cdot C$.

D.HFL: The proposed structure

In fig. 8 is presented the optimal control loop, having as performance criterion the one given in (12). This loop is driven by the high frequency, *turbulence* component and generates the *dynamic* electromagnetic torque, $\Delta\Gamma_G(t)$.

The unique optimal control input minimizing the index expressed in (12) for the dynamic system given by (7) is the full-state feedback law,

$$u(t) = -K \cdot \underline{x}(t) , \tag{13}$$

with the feedback matrix, K, as follows:

$$K = R^{-1} \cdot B^T \cdot S ,$$

where S is the unique, symmetric and positive semi-defined matrix satisfying the Riccati algebraic matrix equation [7]:

$$S \cdot A + A^T \cdot S + C_\alpha^T \cdot C_\alpha - S \cdot B \cdot R^{-1} \cdot B^T \cdot S = 0$$

The closed loop system, described by $\dot{\underline{x}}(t) = \left(A - B \cdot K \right) \cdot \underline{x}(t)$, is asymptotically stable (details of the design procedure can be found in [13]).

IV. Experimental rig

A small scale real time electromechanical simulator of a WECS (fig. 9) has been used to validate the proposed control strategy. The simulator consists in two identical rigidly coupled cage induction machines, one

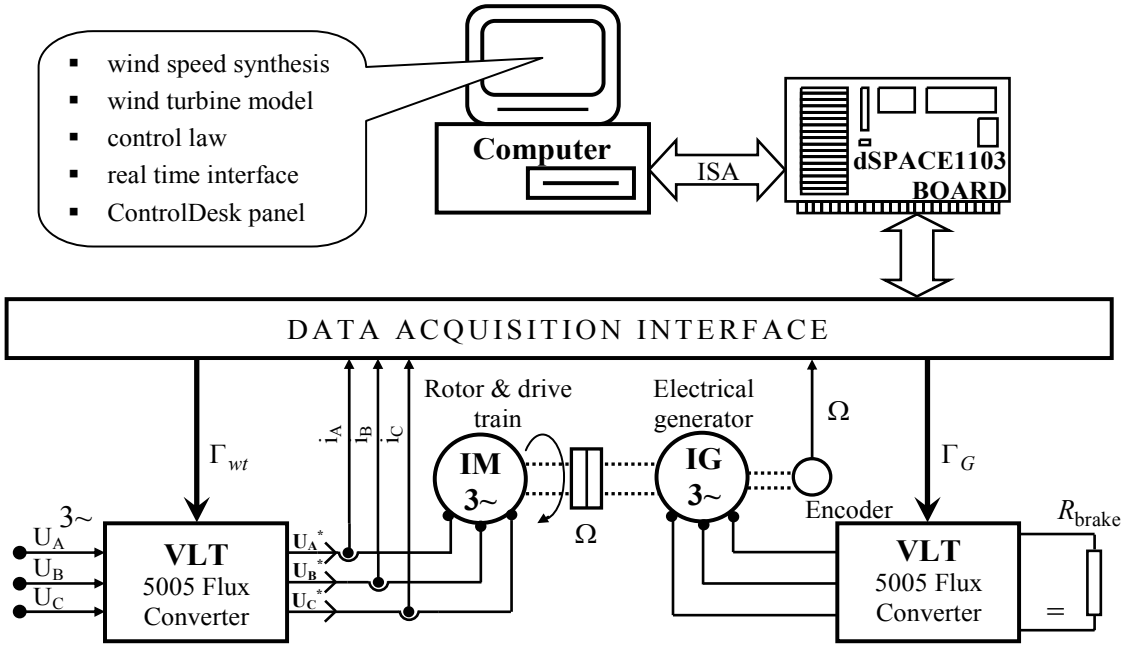

Fig. 9. Hardware structure of the test rig

of which (IM) emulates the aerodynamic subsystem and the drive train of the wind turbine, and the second one (IG) is torque controlled as a generator.

The two induction machines are controlled via power electronics converters, namely VLT 5005 Flux. The computer implements:

- the synthesis of the wind speed, $v(t)$;

- the wind turbine model, utilized to provide the wind torque reference, Γ_{wt} (referred to the high-speed shaft), using the computed wind speed and the real rotational speed, Ω;

- the control law, which provides the generator torque reference, Γ_G.

The simulation schemes have been done under Matlab/Simulink, using Real-Time Interface, and run on the DS1103 PPC controlled board (dSPACE), which is equipped with a Power PC processor for fast floating-point calculation at 400 MHz.

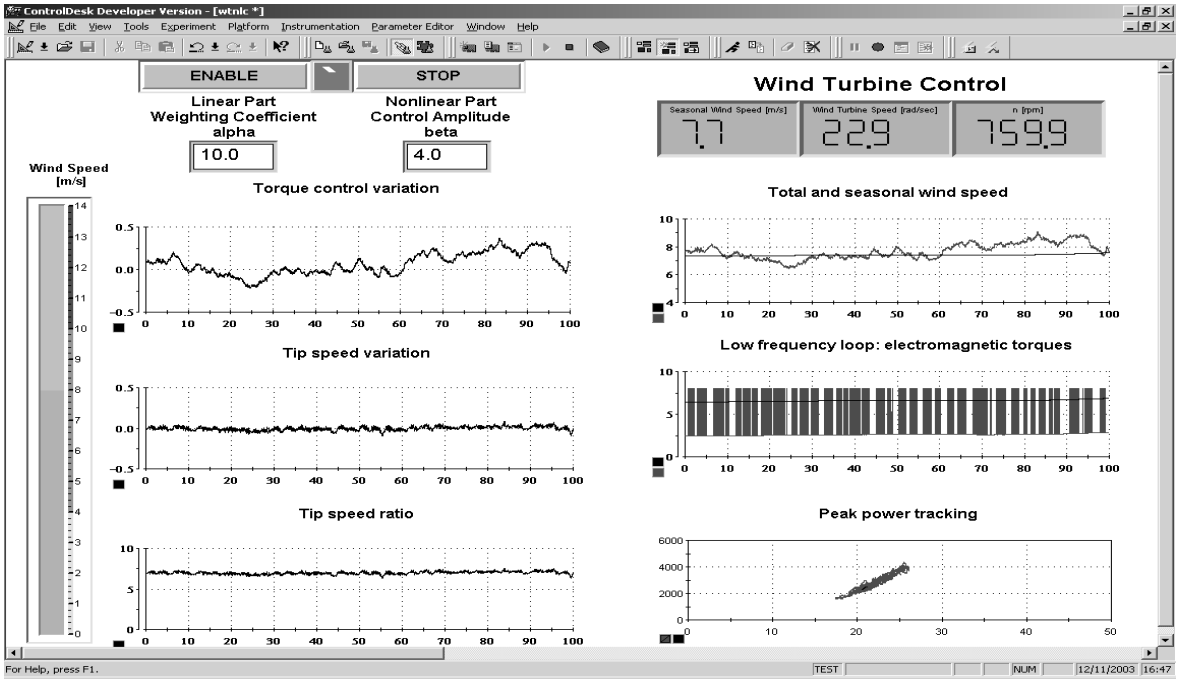

Fig. 10. The ControlDesk panel

The bidirectional information flux between the physical part and the computer is supported by a data acquisition interface. A ControlDesk panel (fig. 10) is used to visualize the functional parameters of the simulated WECS and for getting user-supplied data in real time.

This information concerns mostly control related variables rather than energetic or electromagnetic ones.

V. Experimental results

A. Results concerning the low frequency loop

The bandwidth of the seasonal wind speed which drives the low frequency loop has been limited to 0.1Hz; this speed takes values in the usual range, from 4 to 10 m/s (fig. 11 left). This loop maintains the operating point on the ORC, corresponding to the tip speed of λ_{opt} (7 in our case), as shown in fig. 12 (left side).

Equivalently, the γ parameter is maintained closely around $\gamma(\lambda_{opt}) = -1$ (fig. 11 right), which means that the linearized system (7) is desensitized in relation to this parameter. As the other two parameters, J_T and T_w, present sufficiently weak variations with $\bar{v}$, the system may be considered as invariant.

The tip speed presents sufficiently small oscillations (about 2.5%), whose amplitude depends on the operating point (fig. 12 left).

The electromagnetic torque (right side of fig. 12) is also oscillating, having reasonably small variations around its mean value (about 10%). Practically, these variations are not important to the mechanical stress.

B. Results concerning the high frequency loop

The variables of interest of this loop are normalized variations around a "static operating point", i.e. that of the speed ratio, $z(t) = \overline{\Delta\lambda}(t)$, and that of the generator torque, which is the control input of the liniarized wind power system, $u(t) = \overline{\Delta\Gamma_G}$. In our case, the operating point is maintained on the ORC by the LFL.

Simulations have been performed on the above described test rig for several values of the weighting coefficient, α, and have shown that the performance index values are sensitive to α values in a wide range, approximately between 0.1 and 10. For each value of α, the state feedback, K, is unique and has been computed based upon the model's parameters J_T and T_w, obtained for $\bar{v}$ in the middle of its variation range.

Fig. 13 suggests a qualitative interpretation of the simulation results and shows how the normalized variations of the tip speed ratio and of the electromagnetic torque depend on α. As it was expected, the amplitude of the tip speed ratio normalized variation, $\overline{\Delta\lambda}$, decreases with the value of α, while that of the electromagnetic torque, $\overline{\Delta\Gamma_G}$, increases.

Fig. 14 shows the combined functioning of the two loops, namely the variations of the operating point around the ORC for two values of α. One can note that, for small α (left side), these variations are significantly larger than those for large α (right side). Also, it can be noted that these variations increase as the wind speed increases.

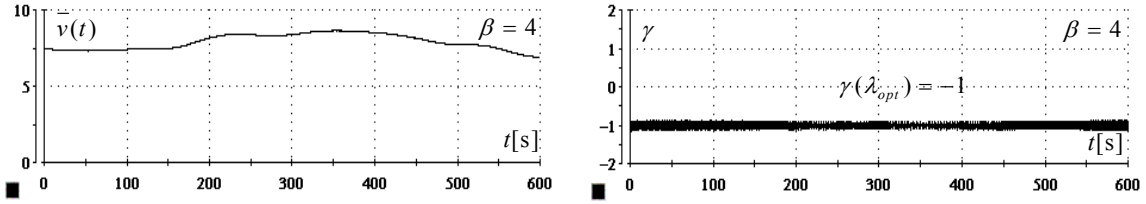

Fig. 11. The evolutions of the seasonal wind speed (left) and of the γ parameter (right)

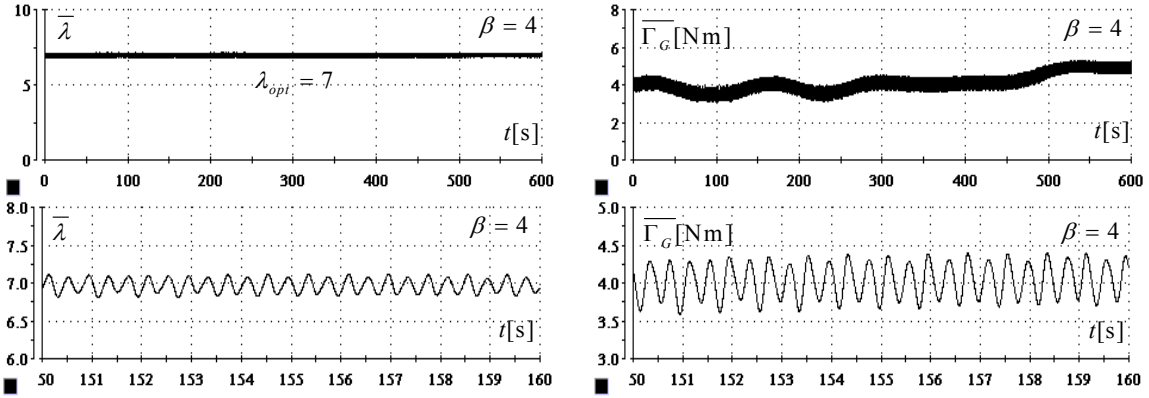

Fig. 12 The evolution of the tip speed ratio (left) and generator torque (right) at different scales

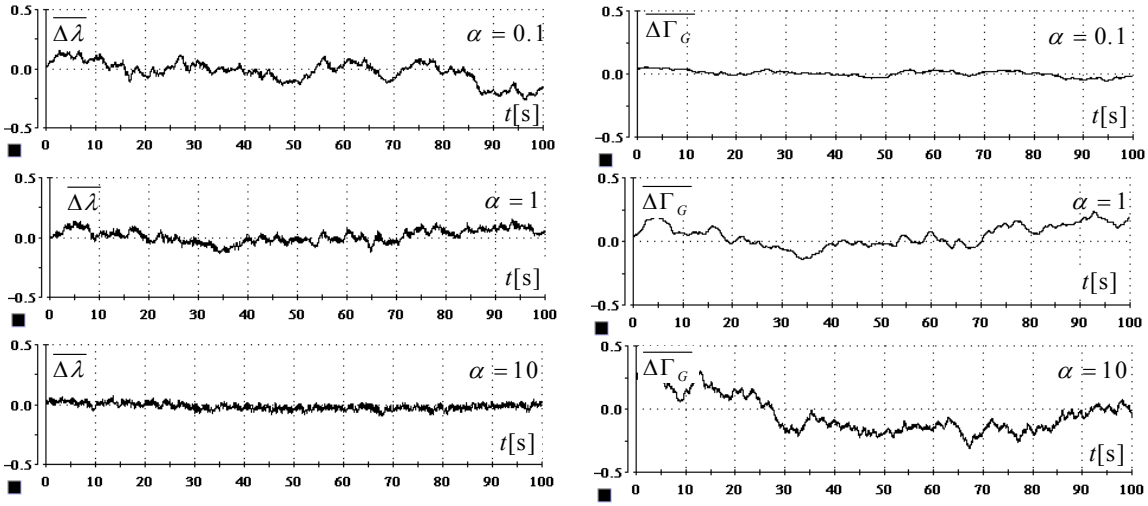

Fig. 13. The evolution of the tip speed ratio (left) and of the generator torque (right) normalized variations for three values of the weighting coefficient α

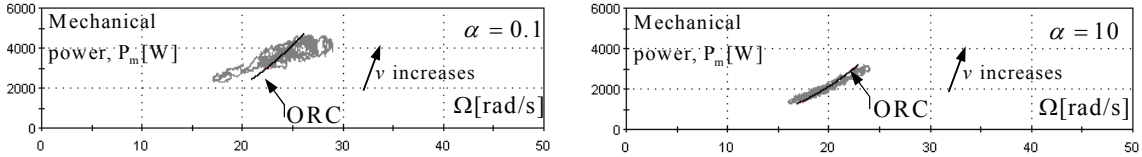

Fig 14. The evolution of the operating point: tracking the ORC

VI. Conclusion

This paper proposes a controller for variable speed fixed pitch wind turbines, whose main goal is to achieve the energetic efficiency improvement. The reliability aspects have also been considered. As a consequence, the controller structure consists in two different loops: the maximum energetic efficiency loop, driven by the low frequency wind speed component, and an energy-reliability trade-off control loop, governed by the turbulence component.

The electric generator is torque controlled, the control input having two components. Its static component is provided by a nonlinear controller, which governs the low frequency loop, whereas the dynamic component results from solving a LQG problem.

The proposed structure offers the possibility of combining the robustness of the nonlinear control with the flexibility of the dynamic optimization law. Indeed, the possibility of varying the weighting coefficient α confers flexibility to the controlled system, so that the wind harvested energy to be significantly increased when the particular conditions of the site allow it, i.e. the mechanical stress induced by the turbulences is not important. On the contrary, if the turbulence is significant, the protection of the drive train can be improved, but this happens in spite of the captured power.

The effectiveness of the presented controller was proved by experimental testing on a small scale real time electromechanical simulator.

Future work will be directed to improving the nonlinear control of the low frequency loop and to generalize the obtained results to other types of WECS.

Acknowledgment

The authors are grateful to Danfoss Denmark for their donation, which has made possible the real time experimentation, and to their colleagues at Aalborg University, Denmark, for their kind advices and support.

References

[1] A. Miller, E. Muljadi, D.S. Zinger, "A Variable Speed Wind Turbine Power Control", *IEEE Transactions on Energy Conversion*, vol. 12(2), pp. 451-457, 1997.

[2] S. Bhowmik, R. Spée, "Wind Speed Estimation Based Variable Speed Wind Power Generation", *Proceedings of the Annual IEEE Conference of the Industrial Electronics Society – IECON'98*, pp. 596-601, Aachen, Germany, 1998.

[3] M.G. Simoes, B.K. Bose, R.J. Spiegel, "Fuzzy Logic Based Intelligent Control of a Variable Speed Cage Machine Wind Generation System", *IEEE Transactions on Power Electronics*, vol. 12(1), 87-95, 1997.

[4] H. De Battista, R.J. Mantz, C.F. Christiansen, "Dynamical Sliding Mode Power Control of Wind Driven Induction Generators", *IEEE Transactions on Energy Conversion*, vol. 15(4), 451-457, 2000.

[5] P. Novak, T. Ekelund, "Modeling, Identification and Control of a Variable Speed HAWT", *Proceedings of the European Wind Energy Conference*, pp. 441-446, Thessaloniki, Greece, 1994.

[6] T. Ekelund, *Modeling and Linear Quadratic Optimal Control of Wind Turbines*. Ph.D. Thesis, Chalmers University of Göteborg, Sweden, 1997.

[7] W.S. Levine (Editor), *The Control Handbook*, CRC Press, 1996.

[8] N.A. Cutululis, I. Munteanu, E. Ceangă, M. Culea, "Optimal control structure for variable speed wind power system",

Proceedings of the 11th National Conference on Electric Drives – CNAE'02, pp. 121-128, Galați, Romania, 2002.

[9] C. Nichita, D. Luca, B. Dakyo, E. Ceangă, "Large Band Simulation of the Wind Speed for Real Time Wind Turbine Simulators", *IEEE Transactions on Energy Conversion*, vol. 17(4), pp. 523-529, 2002.

[10] J. Wilkie, W.E. Leithead, C. Anderson, "Modeling of Wind Turbines by Simple Models", *Wind Engineering*, vol. 4, pp. 247-274, 1990.

[11] C. Nichita, *Étude et développement de structures et lois de commande numériques pour la réalisation d'un simulateur de turbine éolienne de 3 kW*, Thèse de Doctorat, Université du Havre, France, 1995.

[12] T. Burton, D. Sharpe, N. Jenkins, E. Bossanyi, *Wind Energy Handbook*, John Wiley & Sons, 2001.

[13] I. Munteanu, E. Ceangă, N.A. Cutululis, A. Bratcu, "Linear quadratic optimization of variable speed wind power systems", *Preprints of the IFAC Workshop on Control Applications of Optimization – CAO 2003*, pp. 162-167, 30 June – July 2 2003, Visegrád, Hungary.